Cell

Redox Modification of Nuclear Actin by MICAL-2 Regulates SRF Signaling

Mark R. Lundquist,[1] Andrew J. Storaska,[2] Ting-Chun Liu,[3] Scott D. Larsen,[4] Todd Evans,[3] Richard R. Neubig,[2,5] and Samie R. Jaffrey[1,*]

[1]Department of Pharmacology, Weill Cornell Medical College, Cornell University, New York, NY 10065, USA
[2]Department of Pharmacology, University of Michigan, Ann Arbor, MI, 48109, USA
[3]Department of Surgery, Weill Cornell Medical College, Cornell University, New York, NY 10065, USA
[4]Vahlteich Medicinal Chemistry Core, College of Pharmacy, University of Michigan, Ann Arbor, MI 48109, USA
[5]Department of Pharmacology and Toxicology, Michigan State University, East Lansing, MI 48824, USA
*Correspondence: srj2003@med.cornell.edu
http://dx.doi.org/10.1016/j.cell.2013.12.035

SUMMARY

The serum response factor (SRF) binds to coactivators, such as myocardin-related transcription factor-A (MRTF-A), and mediates gene transcription elicited by diverse signaling pathways. SRF/MRTF-A-dependent gene transcription is activated when nuclear MRTF-A levels increase, enabling the formation of transcriptionally active SRF/MRTF-A complexes. The level of nuclear MRTF-A is regulated by nuclear G-actin, which binds to MRTF-A and promotes its nuclear export. However, pathways that regulate nuclear actin levels are poorly understood. Here, we show that MICAL-2, an atypical actin-regulatory protein, mediates SRF/MRTF-A-dependent gene transcription elicited by nerve growth factor and serum. MICAL-2 induces redox-dependent depolymerization of nuclear actin, which decreases nuclear G-actin and increases MRTF-A in the nucleus. Furthermore, we show that MICAL-2 is a target of CCG-1423, a small molecule inhibitor of SRF/MRTF-A-dependent transcription that exhibits efficacy in various preclinical disease models. These data identify redox modification of nuclear actin as a regulatory switch that mediates SRF/MRTF-A-dependent gene transcription.

INTRODUCTION

Serum response factor (SRF) mediates gene transcription induced by serum, various growth factors, and G-protein-coupled receptor signaling pathways (Posern and Treisman, 2006). SRF-dependent gene transcription is modulated by SRF coactivators, including ternary complex factor (TCF) and myocardin-related transcription factor A (MRTF-A) (Shaw et al., 1989; Wang et al., 2002). MRTF-A binds to SRF, forming a complex that influences SRF binding to the CArG box promoter element, which is found in SRF target genes (Miralles et al., 2003; Treisman, 1986). SRF/MRTF-A-dependent gene transcription mediates diverse cellular processes including cellular migration (Leitner et al., 2011), cancer cell metastasis (Brandt et al., 2009; Medjkane et al., 2009), mammary myoepithelium development (Li et al., 2006), and neurite formation (Knöll and Nordheim, 2009; Wickramasinghe et al., 2008).

SRF/MRTF-A-dependent gene transcription is induced when MRTF-A localizes to the nucleus (Posern and Treisman, 2006). MRTF-A is found in both the cytosol and the nucleus but exhibits increased nuclear localization in response to various signaling pathways. The nuclear localization of MRTF-A enables it to form complexes with SRF, resulting in transcription of genes that contain promoter elements that bind the SRF/MRTF-A complex (Posern and Treisman, 2006). Thus, SRF/MRTF-A-dependent gene transcription is highly influenced by the levels of nuclear MRTF-A.

Recent studies have shown that MRTF-A localization is regulated by actin dynamics in the nucleus (Baarlink et al., 2013; Vartiainen et al., 2007). G-actin in the nucleus binds to MRTF-A, enabling it to be exported to the cytosol (Vartiainen et al., 2007). Thus, high levels of G-actin in the nucleus seen during serum deprivation lead to low levels of nuclear MRTF-A. Activation of SRF/MRTF-A-dependent gene transcription occurs when signaling pathways reduce nuclear G-actin, which prevents MRTF-A export, resulting in accumulation of MRTF-A in the nucleus (Vartiainen et al., 2007).

G-actin levels in the nucleus can be regulated by F-actin formation in the cytosol. When actin polymerization is induced in the cytosol, for example following RhoA-induced stress fiber formation, cellular actin becomes sequestered in cytosolic stress fibers, leading to the depletion of G-actin throughout the cell (Vartiainen et al., 2007). RhoA-dependent depletion of G-actin in the nucleus subsequently activates SRF/MRTF-A-dependent gene transcription in NIH 3T3 cells (Vartiainen et al., 2007).

The depletion of monomeric actin by cytosolic stress fibers is unlikely to mediate SRF/MRTF-A signaling in all cell types. For example, SRF/MRTF-A signaling regulates axon growth (Lu and Ramanan, 2011) and other neuronal functions (Knöll and Nordheim, 2009; Wickramasinghe et al., 2008), but stress fiber formation is not typically seen in neurons. Therefore, additional pathways that induce SRF/MRTF-A signaling remain to be identified.

Here, we describe a mechanism that regulates SRF/MRTF-A-dependent gene expression which involves depolymerization of

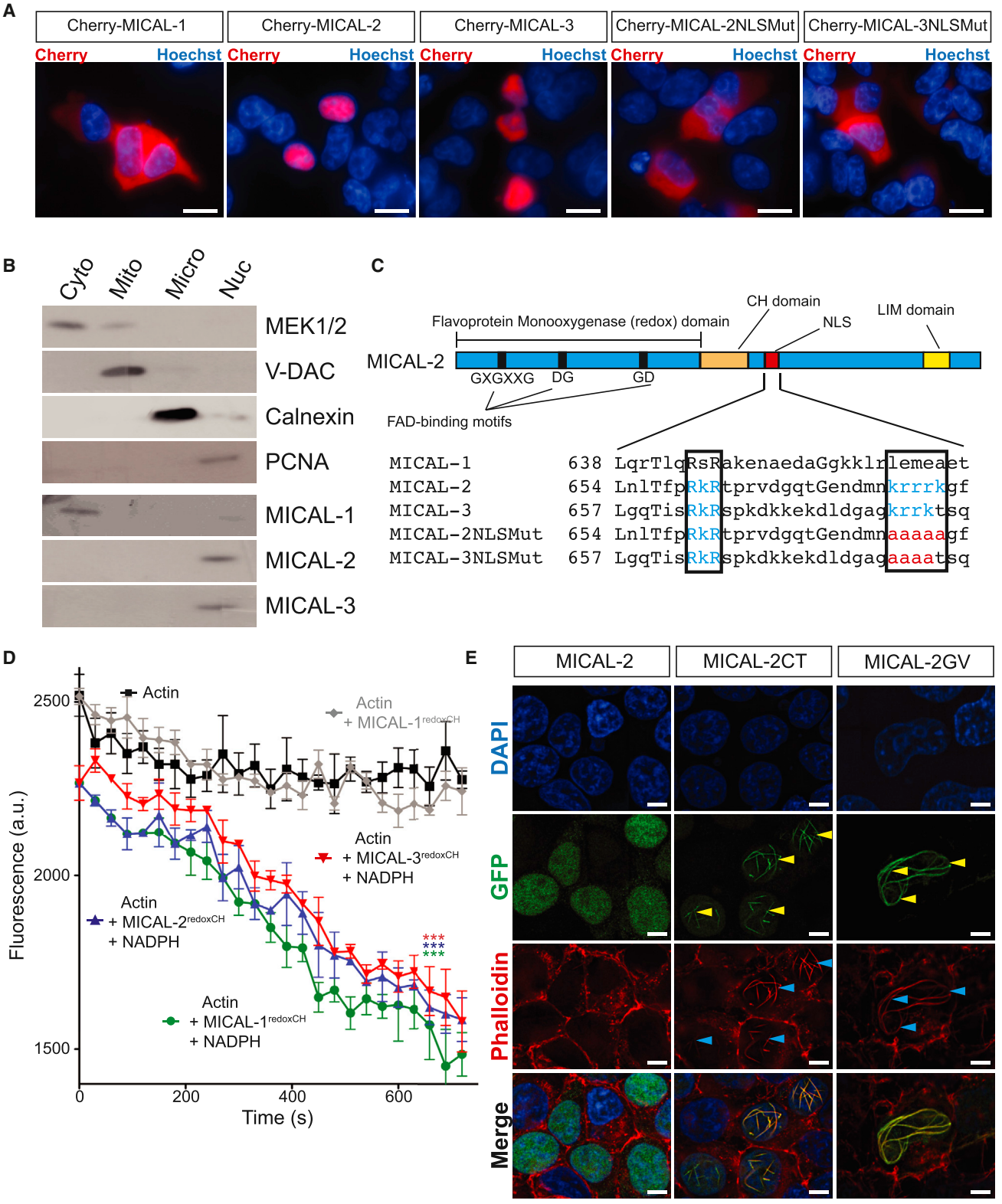

Figure 1. MICAL-2 Is a Nuclear Protein that Depolymerizes Actin

(A) Cherry-MICAL-2 and -3 expressed in HEK293T cells are localized to the nucleus (blue), while Cherry-MICAL-1 and NLS mutant Cherry-MICALs (M2NLSMut and M3NLSMut) exhibited cytosolic localization. Scale bar, 10 μm.

(legend continued on next page)

nuclear actin by MICAL-2, a member of a family of recently described atypical actin-regulatory proteins (Terman et al., 2002). MICAL-2 is homologous to MICAL-1, an enzyme that binds to F-actin in the cytosol and triggers its depolymerization through a redox modification of methionine (Hung et al., 2011; 2010). We show that MICAL-2 is enriched in the nucleus and induces depolymerization of F-actin in the nucleus. Expression of MICAL-2 reduces nuclear actin, resulting in nuclear retention of MRTF-A and subsequent activation of SRF/MRTF-A-dependent gene transcription. We find that MICAL-2 promotes SRF/MRTF-A-dependent gene expression in several cell types, and mediates NGF-dependent neurite growth in neuronal cells. Furthermore, CCG-1423, a small molecule SRF/MRTF-A pathway inhibitor that exhibits efficacy in various preclinical disease models, directly binds MICAL-2 and inhibits its activity. Together, these data show that SRF/MRTF-A signaling is regulated by MICAL-2-dependent redox regulation of nuclear actin.

RESULTS

MICAL-2 Is Enriched in the Nucleus

Because of the important roles of MICAL-1 in depolymerizing actin in axonal growth cones (Hung et al., 2010), we sought to understand if MICAL-2 and -3 have related functions. In order to understand the roles of MICAL-2 and -3, we examined the subcellular localization of each MICAL isoform. Cherry-tagged MICAL-1 was cytoplasmic in HEK293T cells; however, Cherry-MICAL-2 and Cherry-MICAL-3 were nuclear (Figure 1A). To confirm that these localizations are not due to the presence of the Cherry tag, we monitored the localization of endogenous MICALs by subcellular fractionation using isoform-specific antibodies (Figures S1A and S1B available online). MICAL-1 was cytoplasmic, while MICAL-2 and -3 were enriched in the nuclear fraction in HEK293T cells (Figure 1B). The nuclear localization of MICAL-2 was also confirmed by immunofluorescence in HEK293T, COS7, and HeLa cells (Figures S1C and S1D).

The PredictProtein algorithm (Rost et al., 2004) revealed a putative bipartite nuclear localization sequence (NLS) in both MICAL-2 and -3, which was not found in MICAL-1 (Figure 1C). Substitutions in lysine and arginine residues in the NLS abolished the nuclear localization of MICAL-2 and -3 (Figure 1A), confirming that these sequences constitute a NLS domain in these proteins.

MICAL-2 Redox Activity Induces Actin Depolymerization

Because MICAL-2 and -3 share 60% and 63% identity, respectively, with MICAL-1 in the catalytic flavoprotein monooxygenase domain (Terman et al., 2002), we asked if they also depolymerize F-actin. To test this, we purified the bacterially expressed catalytic domain and the adjacent actin-binding calponin homology (CH) domain (designated "redoxCH") for each MICAL isoform (Hung et al., 2010). To measure actin depolymerization, we used a previously described assay for MICAL-1-dependent actin depolymerization using pyrene-labeled actin (Hung et al., 2010). As expected, MICAL-1^{redoxCH}-induced actin depolymerization in an NADPH-dependent manner (Hung et al., 2010) (Figure 1D). Similarly, MICAL-2^{redoxCH} and -3^{redoxCH}-induced actin depolymerization in an NADPH-dependent manner. The rate of NADPH consumption by MICAL-2 and -3 was markedly enhanced by F-actin, suggesting that F-actin is a specific substrate of these enzymes (Figure S1E).

MICAL-2 Regulates Nuclear Actin Polymerization

The ability of MICAL-2 and -3 to depolymerize F-actin in vitro, combined with their nuclear localization, suggests that these isoforms may regulate actin polymerization within the nucleus. We therefore examined the effect of inhibiting MICAL-2 activity on F-actin levels within the nucleus in various cell lines. Expression of either of two dominant-negative MICAL-2 constructs, MICAL-2CT, which contains a deletion of the N-terminal catalytic domain, and MICAL-2GV, which contains a glycine to valine mutation at amino acid 95 that blocks FAD-binding in flavoprotein monooxygenases (Eppink et al., 1997), resulted in marked reorganization of actin into linear filaments that span large portions of the nucleus (Figures 1E and S1F). Similar mutations in MICAL-3 expression constructs did not appear to alter nuclear actin (data not shown).

MICAL-2 knockdown (Figure S1B) resulted in the appearance of nuclear F-actin as detected by phalloidin staining in fixed cells (Figure S1G). Similarly, expression of GFP-tagged LifeAct, which binds to F-actin (Riedl et al., 2008), revealed nuclear F-actin in live cells expressing MICAL-2-specific shRNA (Figure S1H). The MICAL-2 knockdown constructs did not affect cellular viability (Figures S1I and S1J).

To validate that these actin filaments are localized within the nucleus, we costained cells with an antibody to lamin A/C, a marker of the inner nuclear membrane (Figure S1K). Actin filaments were indeed within the nucleus, rather than surrounding

(B) Subcellular fractionation of MICAL isoforms. Endogenous MICAL-2 and -3 are localized to the nucleus while MICAL-1 was detected in the cytosol. MEK1/2, VDAC, Calnexin, and PCNA immunoblotting was used to confirm the purity of the cytosolic (Cyto), mitochondrial (Mito), microsomal (Micro), and nuclear (Nuc) fractions, respectively.

(C) MICAL-2 and -3 each contain a putative bipartite NLS. The domain structure of MICAL-2 is indicated above. The enzymatic domain contains a GXGXXG, aspartate-glycine (DG), and a glycine-aspartate (GD) motif, which is the characteristic FAD-binding motif. The F-actin-binding CH domain and LIM domain are indicated. A potential bipartite NLS (red box) in MICAL-2 and MICAL-3 is not found in MICAL-1. Shown in blue letters are the amino acids that constitute the NLS in MICAL-2 and -3. Shown in red are the amino acids that are mutated in the M2NLSMut and M3NLSMut. Uppercase letters are amino acids conserved in MICAL-1, -2 and -3.

(D) MICAL-2 and -3 depolymerize F-actin similarly to MICAL-1. MICAL-1^{redoxCH}, MICAL-2^{redoxCH} and MICAL-3^{redoxCH} were incubated with pyrene-labeled actin and NADPH as indicated. These data indicate that MICAL-2 and MICAL-3, like MICAL-1, induce NADPH-dependent F-actin depolymerization. Statistical significance was determined by one-way analysis of variance (ANOVA) (***$p < 0.0007$) with Dunnett multiple comparison posttest. ***$p < 0.0005$, $n \geq 12$. Mean ± SEM.

(E) Dominant-negative inhibition of MICAL-2 lead to increased nuclear F-actin. Expression of dominant-negative MICAL2 (MICAL-2CT or MICAL-2GV, green) resulted in the appearance of filaments (yellow arrows) throughout the nucleus (blue), as seen by phalloidin labeling (red staining, blue arrows). The dominant-negative constructs colocalized with the F-actin (yellow). Scale bar, 5 μm.

See also Figure S1

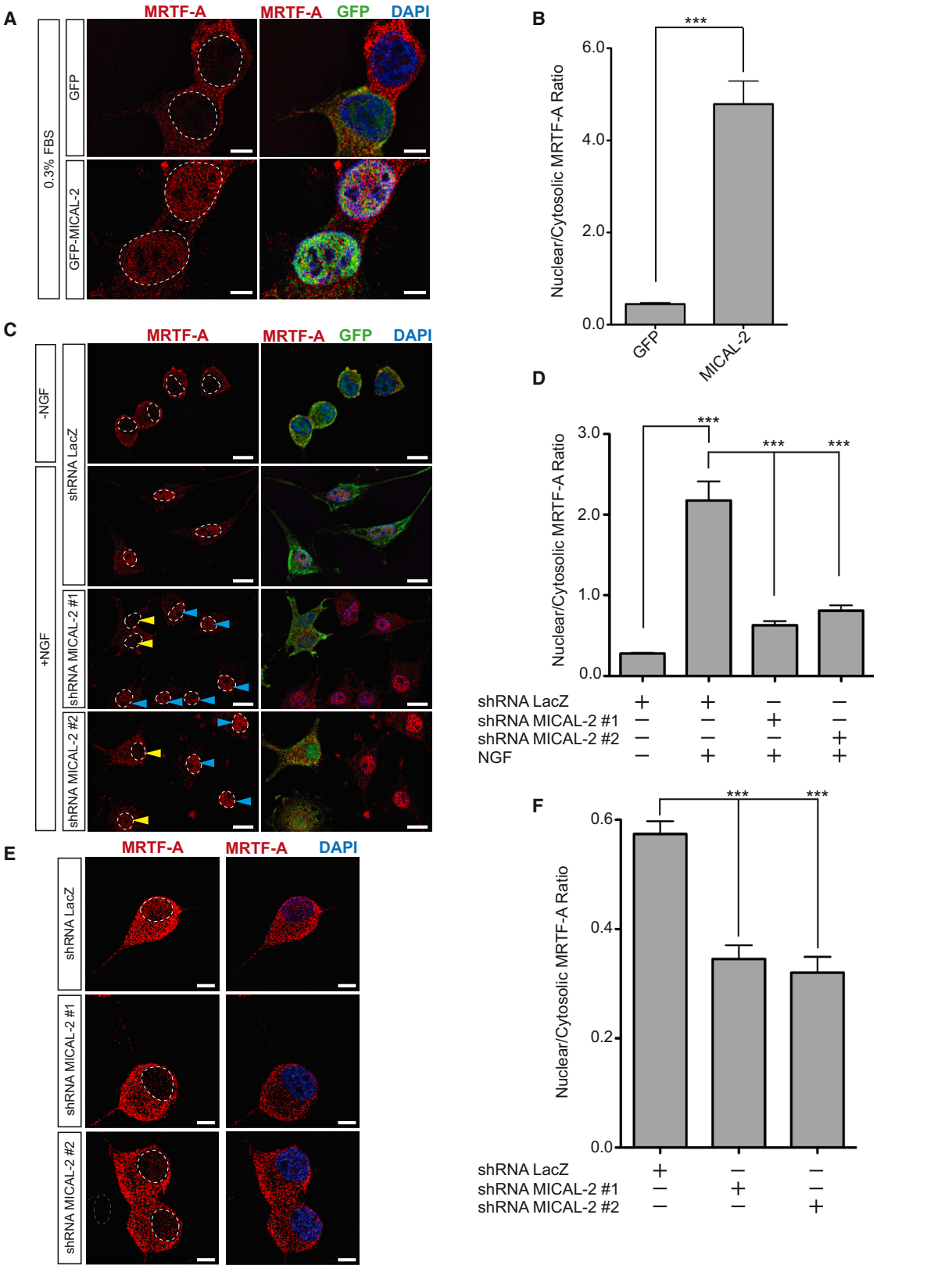

(legend on next page)

the nuclear membrane (Figures S1L–S1O). Collectively, these data indicate that MICAL-2 enzymatic activity inhibits polymerization of nuclear actin in cells.

MICAL-2 Expression Induces Nuclear Localization of MRTF-A

Since MICAL-2 regulates F-actin within the nucleus, and since nuclear G-actin mediates nuclear export of MRTF-A (Vartiainen et al., 2007), we considered the possibility that MICAL-2 reduces nuclear MRTF-A by promoting its export. To test this, HEK293T cells were infected with a virus expressing either GFP or GFP-MICAL-2 and serum-starved for 18 hr under low-serum conditions (0.3% fetal bovine serum [FBS]) (Miralles et al., 2003) (Figures 2A and 2B). Contrary to our expectation, overexpression of MICAL-2 under these conditions caused a marked increase in nuclear localization of MRTF-A (Figures 2A and 2B).

We next asked whether the nuclear localization of MRTF-A induced by serum is mediated by MICAL-2. Treatment of serum-starved HEK293T cells with 10% FBS for 10 min altered MICAL-2 phosphorylation levels, suggesting that serum may regulate the function of MICAL-2 (Figures S2A and S2B). To determine whether MICAL-2 is required for serum-mediated accumulation of MRTF-A in the nucleus, we monitored MRTF-A localization following knockdown of MICAL-2. In HEK293T cells expressing either of two MICAL-2-specific shRNAs, but not control shRNA, serum-induced localization of MRTF-A to the nucleus was markedly reduced (Figures S2C and S2D). Thus, MICAL-2 induces nuclear localization of MRTF-A in the absence of serum stimulation and is required for the increase in nuclear MRTF-A levels after serum stimulation.

We considered the possibility that MICAL-2 could increase nuclear MRTF-A by increasing expression levels of MRTF-A. However, MICAL-2 expression has no discernable effect on global levels of MRTF-A (Figure S2E). Additionally, the nuclear accumulation of MRTF-A does not appear to reflect binding of MRTF-A to MICAL-2 (Figures S2F and S2G). Lastly, expression of MICAL-2 did not induce stress fibers or increase cytosolic F-actin levels in HEK293T cells (Figures S2I–S2L). Thus, MICAL-2 does not increase nuclear MRTF-A by increasing cytosolic F-actin.

MICAL-2 Mediates NGF-Dependent Nuclear Localization of MRTF-A

We next examined whether MICAL-2 is required for nuclear localization of MRTF-A after growth factor stimulation. MRTF-A was readily detectable in the cytosol in untreated PC12 cells and exhibited increased nuclear localization in response to NGF treatment (Figures 2C and 2D). However, MRTF-A nuclear localization in response to NGF was markedly reduced by expression of either of two MICAL-2-specific shRNAs, but not by a control shRNA (Figures 2C and 2D).

We next asked whether MICAL-2 promotes the nuclear localization of MRTF-A in primary neurons. For these experiments, we used rat embryonic day (E) 14 dorsal root ganglia (DRG) sensory neurons, which are typically cultured in NGF. Because these neurons require NGF for survival (Chun and Patterson, 1977), we did not test culture conditions lacking NGF. In these neurons, MRTF-A was readily detectable in both the nucleus and cytoplasm (Figures 2E and 2F). Infection of these cells with lentivirus expressing either of two MICAL-2-specific shRNAs resulted in a marked decrease in nuclear MRTF-A (Figures 2E and 2F). Taken together, these data indicate that MICAL-2 is required for efficient nuclear localization of MRTF-A.

MICAL-2 Expression Induces the SRF/MRTF-A-Dependent Reporter

Because MICAL-2 induces nuclear localization of MRTF-A, we asked whether MICAL-2 activates SRF/MRTF-A-dependent gene transcription. To test this, we determined the effect of MICAL-2 expression on a transcriptional reporter containing luciferase under the control of a CArG [$CC(A/T)_6GG$] element. In serum-starved HEK293T cells, minimal levels of luciferase were detected (Figure 3A). However, expression of MICAL-2 resulted in a 15-fold increase in luciferase expression (Figure 3A). This effect was not seen following expression of MICAL-2 mutants that were catalytically inactive or which contain NLS mutations (Figure 3A). MICAL-2 did not induce a transcriptional reporter containing the highly related TCF/ETS SRE element, which requires SRF, but not MRTF-A (Buchwalter et al., 2004) (Figure 3B). Collectively, these data indicate that MICAL-2 induces SRF/MRTF-A-dependent reporter gene expression.

MICAL-1 and MICAL-3 overexpression did not activate the reporter, indicating that activation of SRF/MRTF-A-dependent gene expression is limited to MICAL-2 in HEK293T cells (Figure 3C, S3A, and S3B).

To confirm that MICAL-2-mediated activation of SRF/MRTF-A gene transcription requires MRTF-A, we expressed MRTF-A-ΔTAD, a dominant-negative MRTF-A mutant. This protein lacks the transcription activation domain (TAD) that is necessary for an active SRF/MRTF-A complex (Wang et al., 2003). Expression

Figure 2. MICAL-2 Induces the Nuclear Localization of MRTF-A

(A) MICAL-2 expression (green) induces nuclear localization of MRTF-A (red) under serum-starvation. Nuclei are outlined in white, based on DAPI staining (blue). Scale bar, 5 μm.

(B) Quantification of (A). The average intensity of MRTF-A immunofluorescence was quantified in the nucleus and the cytoplasm. The nucleus:cytoplasmic ratio of MRTF-A increased 10.76-fold in GFP-MICAL-2-expressing cells compared to GFP-expressing cells. ***$p < 0.0005$, Student's t test, $n \geq 30$.

(C) MICAL-2 is required for NGF-induced nuclear localization of MRTF-A in PC12 cells. NGF treatment induces nuclear localization of MRTF-A in *LacZ* shRNA-expressing PC12 cells. PC12 cells expressing *MICAL-2*-specific shRNA (yellow arrows) showed reduced NGF-induced nuclear localization of MRTF-A compared to uninfected cells (blue arrows). Nuclear border indicated by dotted white lines. Scale bar, 10 μm.

(D) Quantification of (C). ***$p < 0.0005$, ANOVA (***$p < 0.0001$) with Dunnett posttest $n \geq 30$. All data in this figure are mean ± SEM.

(E) The nuclear localization of MRTF-A in dissociated E14 DRG neurons cultured in the presence of NGF is dependent upon MICAL-2. Infection of DRG neurons with MICAL-2-specific shRNA results in a substantial nuclear depletion of MRTF-A (red). Scale bar, 5 μm.

(F) Quantification of (E). ANOVA (***$p < 0.0005$) with Dunnett posttest. $n \geq 25$.

See also Figure S2.

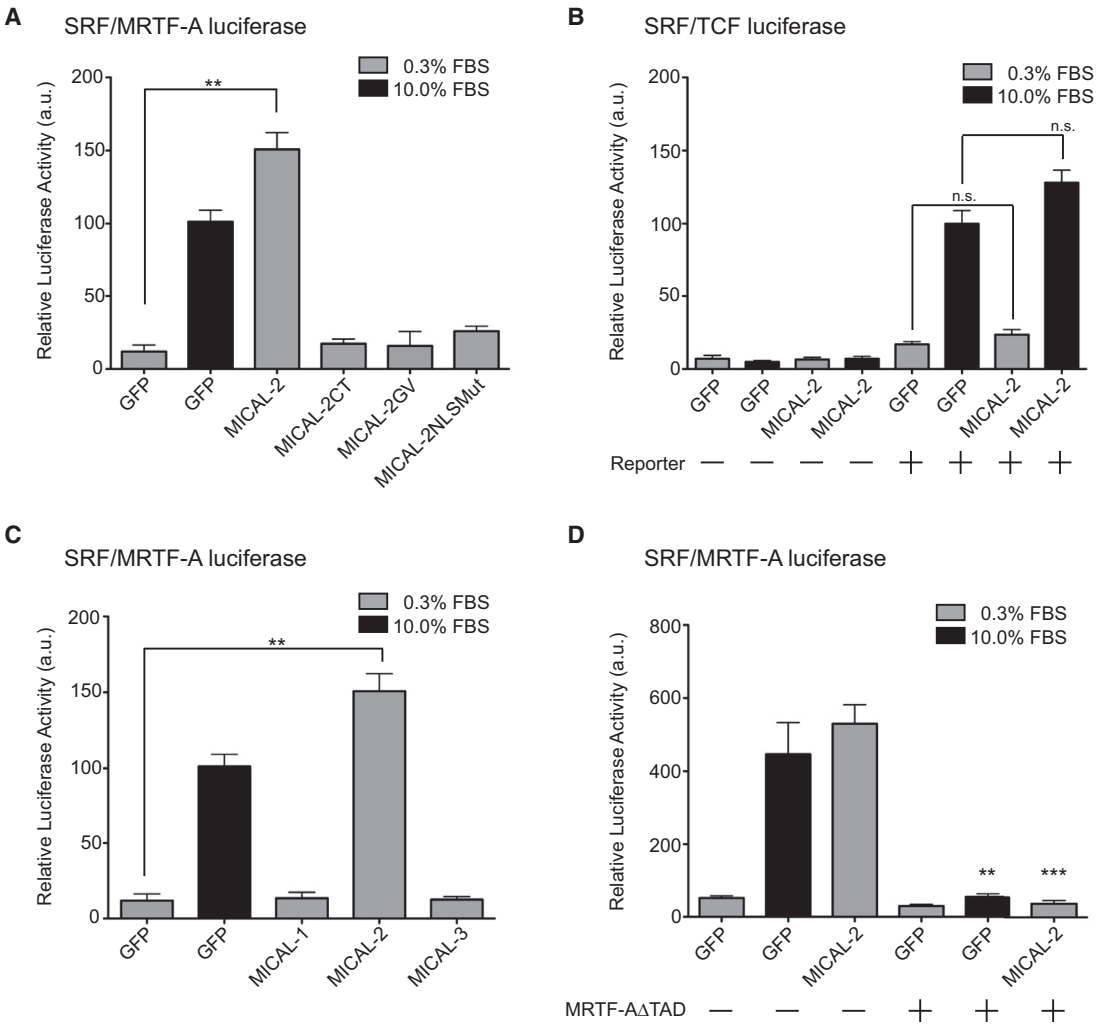

Figure 3. MICAL-2 Induces SRF/MRTF-A-Mediated Luciferase Expression

(A) MICAL-2 induces the SRF/MRTF-A transcriptional reporter in serum-starved (0.3% FBS)-treated cells. Catalytically inactive MICAL-2 mutants (MICAL-2GV and MICAL-2CT), as well as a MICAL-2 mutant that does not localize to the nucleus (M2NLSMUT) does not induce the reporter. ANOVA (**$p < 0.005$) with Dunnett posttest. n = 18. All data in this figure are mean ± SEM.

(B) MICAL-2 does not activate the MRTF-A-independent SRF/TCF luciferase promoter. ANOVA (***$p < 0.0001$) with Dunnett posttest. n = 18.

(C) MICAL-2, but not MICAL-1 or MICAL-3, activates the SRF/MRTF-A luciferase reporter. ANOVA (***$p < 0.0005$) with Dunnett posttest. n = 18.

(D) MICAL-2-dependent induction of the SRF/MRTF-A reporter requires MRTF-A. Coexpression of dominant-negative MRTF-AΔTAD blocked MICAL-2-dependent induction of luciferase. ANOVA (***$p < 0.0001$) with Dunnett posttest. n = 18.

See also Figure S3.

of MRTF-A-ΔTAD blocked the effect of MICAL-2 on the SRF/MRTF-A reporter (Figure 3D). Thus, MICAL-2 induces the reporter in an MRTF-A-dependent manner.

MICAL-2 Expression Induces Endogenous SRF/MRTF-A Target Gene Expression

We next asked whether MICAL-2 induces endogenous SRF/MRTF-A target genes. SRF/MRTF-A target genes have been validated in numerous cell lines (Medjkane et al., 2009; Selvaraj and Prywes, 2004) and neuronal cells (Knöll and Nordheim, 2009). Expression of MICAL-2 in serum-starved HEK293T cells resulted in increased levels of several known SRF/MRTF-A target genes in these cells by 30%–50%, including *Acta2*, *Cyr61*, *SRF*, and *VCL* (Figure S4A). Expression of MICAL-2 had a negligible effect on MRTF-A-independent SRF-dependent genes that contain the TCF/ETS SRE element in their promoter *TSP1*, *PTGS1*, and *Egr2*.

Expression of MICAL-2 in PC12 cells similarly induced SRF/MRTF-A target genes *Acta2*, *Cyr61*, and *SRF* by 100%–200% (Figure S4C). MICAL-2 expression did not induce SRF-dependent, MRTF-A-independent genes, such as *TSP1*, *PTGS1*, and *Egr2* (Figure S4C). These data indicate that MICAL-2 expression induces endogenous SRF/MRTF-A-dependent gene expression.

MICAL-2 Is Required for Serum and NGF-Induced SRF/MRTF-A Target Gene Expression

We next examined whether MICAL-2 mediates the induction of SRF/MRTF-A target genes in response to serum and NGF. In fibroblasts, serum induces the expression of *Acta2*, *Cyr61*, *VCL*, and *SRF* in an SRF- and MRTF-A-dependent manner (Descot et al., 2009; Lee et al., 2010) (Figure S4B). However, expression of either of two *MICAL-2*-specific shRNAs blocked this effect (Figure S4B). *MICAL-2*-specific shRNAs did not affect the induction of MRTF-A-independent SRF-dependent genes *TSP1*, *PTGS1*, and *Egr2*. In PC12 cells, NGF induces the expression of *Acta2*, *Cyr61*, *VCL*, and *SRF* in an SRF- and MRTF-A-dependent manner (Figure S4D). *MICAL-2* shRNAs impaired NGF-induced expression of these SRF/MRTF-A target genes (Figure S4D) but did not affect NGF-mediated induction of MRTF-A-independent SRF-dependent genes *TSP1* and *PTGS1*. Similarly, rat E14-15 DRG neurons cultured in NGF exhibited a reduction in *Acta2*, *Cyr61*, and *VCL* expression upon infection with lentivirus expressing either of two *MICAL-2* shRNAs, while MRTF-A-independent SRF-dependent genes *TSP1*, *PTGS1*, and *Egr2* were unchanged (Figure S4E). Thus, MICAL-2 promotes serum- and NGF-dependent increases in SRF/MRTF-A-dependent gene expression.

MICAL-2 Is Required for NGF-Dependent Neurite Outgrowth

To further address whether MICAL-2 mediates NGF-induced SRF/MRTF-A-dependent transcription, we monitored the effect of MICAL-2 knockdown on NGF-dependent neurite outgrowth in PC12 cells and embryonic DRG sensory neurons. In PC12 cells expressing *MICAL-2*-specific shRNA, neurite length 4 days after NGF treatment was reduced by ~40% compared to *LacZ* shRNA-infected PC12 cells (Figures 4A and 4B). Knockdown of *MICAL-2* in differentiated PC12 cells also decreases neurite formation after NGF treatment (Figure 4C). Similar to PC12 cells, DRG neurons expressing *MICAL-2*-specific shRNA exhibited a ~45% decrease in axon growth rate at DIV5 compared to LacZ-shRNA expressing neurons (Figures 4D and 4E). Taken together, these data indicate that MICAL-2 mediates NGF-induced SRF/MRTF-A signaling in both PC12 cells and primary embryonic sensory neurons.

Embryonic MICAL-2 Knockdown Impairs SRF/MRTF-A-Dependent Gene Expression

We next asked whether MICAL-2 mediates SRF/MRTF-A-dependent gene transcription induced by physiologic signals. SRF-dependent gene transcription is required for heart development in zebrafish (Chong et al., 2012). MICAL isoforms have been characterized in zebrafish (Xue et al., 2010), with the cardiac-enriched *mical2b* exhibiting highest sequence identity to mouse MICAL-2.

We therefore knocked down *mical2b* during embryonic development using antisense morpholinos (Figures S5A and S5C). We used either a splice-blocking morpholino or a translation-blocking morpholino and injected them into developing embryos at the 1-cell stage. Depletion of *mical2b* transcripts by the splice-blocking morpholino was validated by qRT-PCR (Figure S5B). Knockdown of *mical2b* resulted in small hearts that failed to undergo normal looping at 24 hpf (Figures 5A and 5B), with thin, linear morphology compared to wild-type hearts at 48 hpf (Figures 5C and 5D). Additionally, cardiomyocytes in morphant hearts were spatially disorganized, rather than displaying the relatively even distribution seen in wild-type hearts, as shown at 52 hpf in the atria (Figures 5E–5G). Taken together, these data confirm that *mical2b* expression was effectively knocked down in zebrafish.

We next asked whether *mical2b*-deficient animals exhibited selective defects in SRF/MRTF-A-dependent gene transcription. We found that many cardiac muscle-specific SRF/MRTF-A target genes, such as *cardiac alpha actin*, *smooth muscle alpha actin*, *cardiac actin smooth muscle*, *skeletal alpha actin*, *smooth muscle 22a*, *srf*, and *calponin* (Chong et al., 2012; Davis et al., 2008; Descot et al., 2009) were markedly reduced in *mical2b* knockdown animals (Figure 5H). The control genes *vascular endothelial growth factor* (*vegf*), *fibroblast growth factor 4* (*fgf4*), and *ETS translocation variant 4* (*pea3*), which regulate MRTF-A-independent cardiac development in zebrafish, were not affected by *mical2b* knockdown (Figure 5H) (Liang et al., 2001; Znosko et al., 2010). Coinjection of the morpholinos with RNA encoding full-length human MICAL-2, but not MICAL-2GV, normalized expression of the SRF/MRTF-A-dependent genes (Figure 5H). Thus, *mical2b* regulates SRF/MRTF-A-dependent gene transcription in response to physiological stimuli during zebrafish development.

MICAL-2 Does Not Activate SRF/MRTF-A through RhoA

We considered the possibility that MICAL-2 activates SRF/MRTF-A signaling by increasing RhoA activity. However, application of cell-permeable C3-transferase, an inhibitor of RhoA, or Y-27632, a ROCK inhibitor, did not block MICAL-2-induced activation of the SRF/MRTF-A reporter in serum-starved HEK293T cells (Figure 6A) or MICAL-2-dependent MRTF-A nuclear accumulation (Figure 6B). These data, along with our finding that MICAL-2 does not affect cytosolic F-actin levels (Figures S2I–S2L), indicate that MICAL-2 does not activate SRF/MRTF-A reporter expression through the RhoA pathway.

MICAL-2 Induces Depletion of Nuclear Actin

We next asked if MICAL-2 activates SRF/MRTF-A-dependent gene transcription by depleting nuclear G-actin. To test this, we measured nuclear actin levels in HEK293T cells with Alexa 594-DNase I, which specifically binds G-actin (Suck et al., 1981). Consistent with previous studies (Mouilleron et al., 2011; Vartiainen et al., 2007), we found that serum-starvation was associated with higher G-actin levels in the nucleus than in the cytoplasm (Figures 6C and 6D). MICAL-2 overexpression caused a significant reduction in nuclear G-actin, even in the absence of serum (Figures 6C and 6D). The reduction in nuclear G-actin induced by MICAL-2 was similar to the reduction induced by serum stimulation (Figures 6C and 6D). These data suggest that MICAL-2 induces nuclear localization of MRTF-A by reducing nuclear G-actin levels.

We next asked if MICAL-2 promotes the reduction in nuclear G-actin seen after NGF stimulation. In differentiated PC12 cells, NGF induced a significant decrease in nuclear G-actin (Figures S6A and S6B). Expression of GFP-MICAL-2 in unstimulated

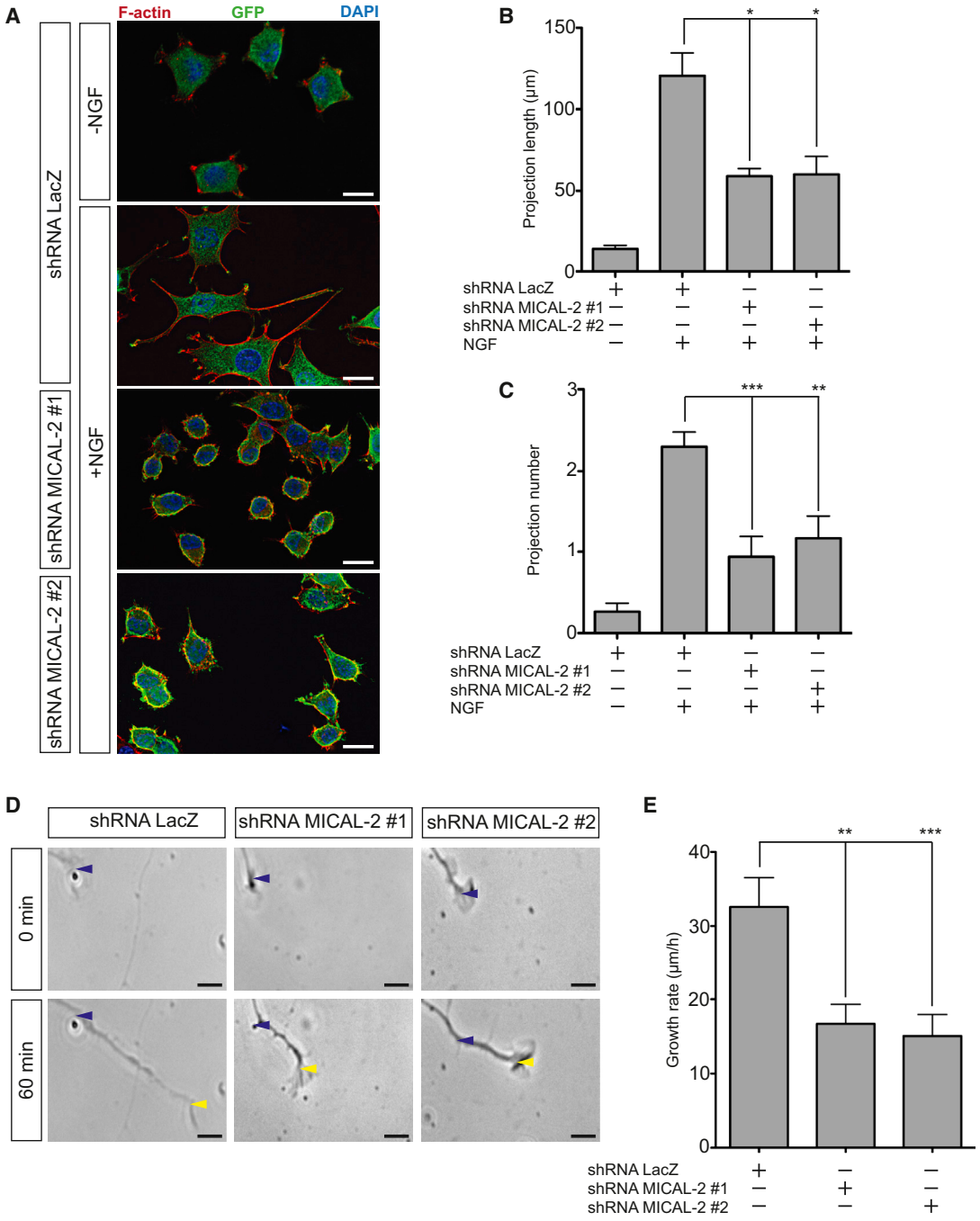

Figure 4. MICAL-2 Is Required for NGF-Dependent Neurite Outgrowth in PC12 Cells and DRG Neurons

(A) MICAL-2 is required for NGF-induced neurite outgrowth in PC12 cells. NGF treatment (50 ng/ml) for 48 hr resulted in prominent neurite outgrowth in LacZ shRNA (green) control as measured by Alex568-phalloidin staining (red). Knockdown of MICAL-2 with either of two shRNA significantly reduces neurite outgrowth. Scale bar, 10 μm.

(B) Quantification of neurite length in (A). The average length of all neurite extensions were quantified in LacZ shRNA- and MICAL-2 shRNA-expressing PC12 cells. ANOVA (***$p < 0.0001$) with Dunnett posttest. *$p < 0.05$, $n \geq 40$. All data in this figure are mean ± SEM.

(C) Quantification of neurite number in (A). Knockdown of MICAL-2 significantly reduced the average number of neurites induced by NGF treatment. ANOVA (***$p < 0.0001$) with Dunnett posttest. ***$p < 0.0005$, **$p < 0.005$, $n \geq 40$.

(D) MICAL-2 knockdown decreases axon growth rates in DRG neurons. DRG neurons expressing either LacZ-specific or MICAL-2-specific shRNA were imaged at 0 (blue arrow) and 60 min (yellow arrow). Scale bar, 10 μm.

(E) Quantification of rates in D. ANOVA (***$p < 0.0004$) with Dunnett posttest. ***$p < 0.0005$, **$p < 0.005$, $n \geq 20$.

See also Figure S4 and Table S1.

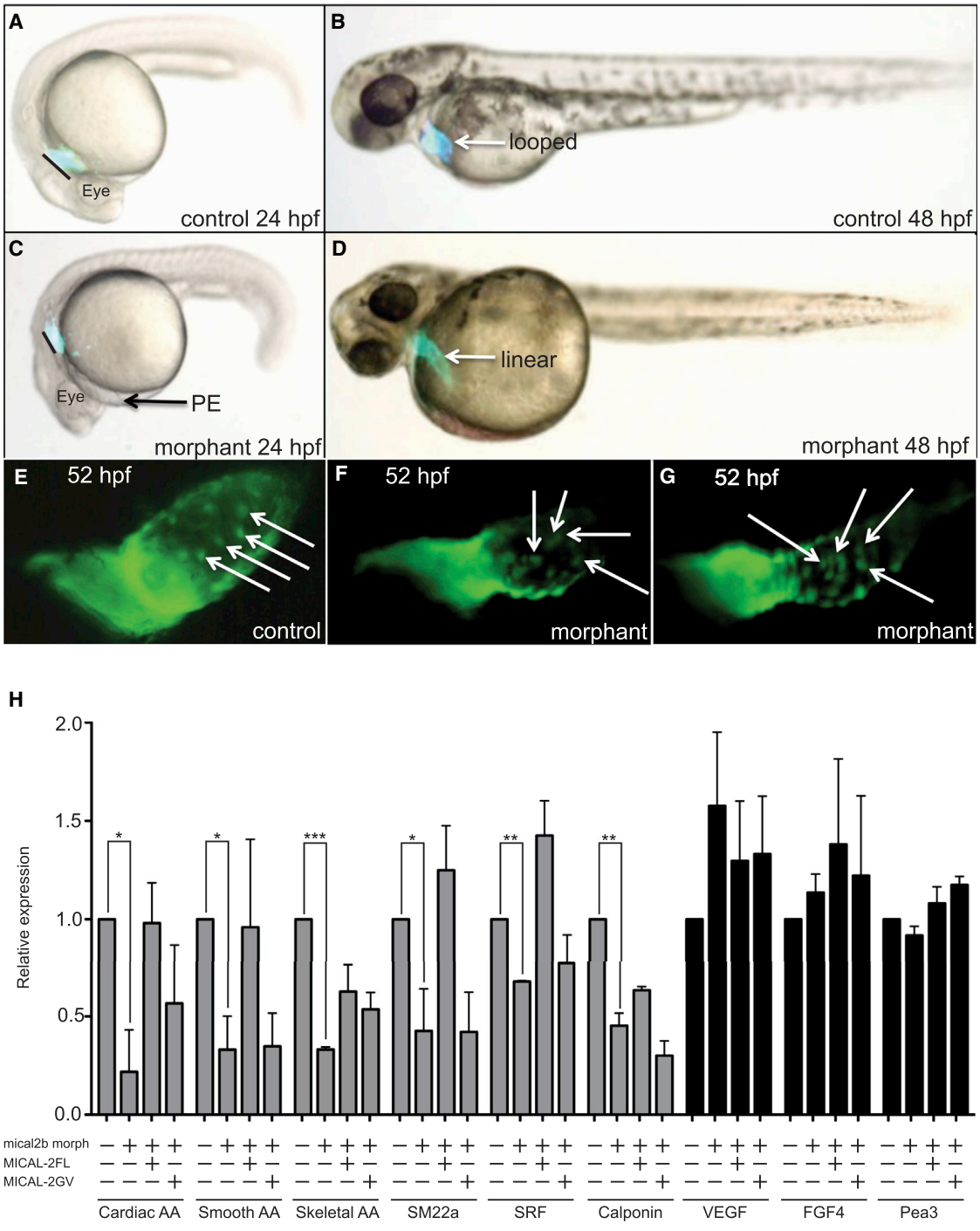

Figure 5. MICAL-2 Regulates SRF/MRTF-A-Dependent Gene Transcription during Zebrafish Development

(A,B) Representative control embryo derived from transgenic *myl7:egfp* reporter fish at 24 hpf, showing the size and position of a normal looping heart tube. By 48 hpf the control heart is fully looped. The *myl7:egfp* transgene directs eGFP expression to myocardial cells and facilitates detection of alterations in heart morphology.

(C,D) *mical2b* regulates cardiogenesis during zebrafish development. The *mical2b* splice-blocking morphant embryo at 24 hpf shows a smaller heart tube that fails to loop normally and thus is positionally displaced and leads to a significant pericardial edema (PE). By 48 hpf the morphant heart tube is linear and dysmorphic. Similar results were obtained with the translation blocking morpholino. For A-D n > 100.

(E) Higher magnification view of the normal control heart at 52 hfp highlights the evenly spaced cardiomyocytes (white arrows) focused on the atrial chamber.

(F-G) In contrast, cells in the smaller morphant atrium are irregularly spaced (white arrows). The representative embryonic hearts shown in F and G are for embryos injected with 2 or 4 ng of the splice-blocking morpholino, respectively (n > 50).

(legend continued on next page)

PC12 cells also induced a significant decrease in the ratio of nuclear:cytosolic G-actin (Figures S6A and S6B). Furthermore, in PC12 cells expressing either of two MICAL-2-specific shRNAs, NGF-dependent reduction in nuclear G-actin levels was significantly impaired (Figures S6C and S6D). Consistent with these findings, DRG neurons expressing either of two *MICAL-2*-specific shRNAs exhibited significantly increased nuclear G-actin levels (Figures S6E and S6F). These data suggest that MICAL-2 mediates NGF-induced reductions in nuclear G-actin.

We next asked if the effects of MICAL-2 were due to a direct effect on actin. MICAL-1 oxidizes methionine 44 in actin to form methionine sulfoxide (Hung et al., 2011). We therefore asked whether a M44Q substitution, which mimics features of the oxidized form of actin, alters actin localization in cells. Wild-type GFP-actin was largely cytosolic though a small portion was found in the nucleus (Figures S6G and S6H). However, GFP-actin M44Q was significantly excluded from the nucleus. On the other hand, GFP-actin M44L, which is not oxidizable, exhibited higher nuclear levels than wild-type actin (Figures S6G and S6H). These data suggest that oxidation of Met44 promotes exclusion of actin from the nucleus. GFP-actin and GFP-actin M44L colocalized with phalloidin staining at similar levels; however, GFP-actin M44Q colocalization with phalloidin was significantly reduced (Figure S6I). The lack of incorporation of GFP-actin M44Q in F-actin is consistent with the known depolymerizing effect of MICAL-2 on actin. We next asked whether oxidation of actin methionine 44 is required for MICAL-2-dependent reduction in nuclear G-actin. To test this, we monitored the effect of MICAL-2 on nuclear localization of GFP-actin and GFP-actin M44L. In these experiments we found that MICAL-2 coexpression decreased nuclear GFP-actin, but not GFP-actin M44L (Figures 6E and 6F). These data suggest that MICAL-2-dependent oxidation of methionine 44 leads to a reduction in nuclear G-actin.

The SRF/MRTF-A Pathway Inhibitor CCG-1423 Is a MICAL-2 Inhibitor

CCG-1423 is a small molecule inhibitor of SRF/MRTF-A-dependent transcription that was identified in a cell-based screen using a SRF/MRTF-A reporter (Evelyn et al., 2007). While CCG-1423 has shown utility in preclinical disease models, its specific molecular target is not known.

CCG-1423 treatment reduces nuclear MRTF-A levels (Jin et al., 2011), which is similar to the effect of MICAL-2 knockdown (Figures 2C–2F and Figures S2C and S2D). Therefore, we wondered whether the effects of CCG-1423 on SRF/MRTF-A signaling are mediated by inhibition of MICAL-2. As a first test, we asked whether CCG-1423 blocks MICAL-2 signaling in cells. In this experiment, we monitored the effect of CCG-1423 on MICAL-2-dependent induction of the SRF/MRTF-A reporter in serum-starved HEK293T cells. Expression of MICAL-2-induced luciferase expression, while treatment with 5 μM CCG-1423 for 4 hr reduced it by 75% ($p < 0.001$, Figure 7A). These data indicate that CCG-1423 blocks MICAL-2-mediated induction of the SRF/MRTF-A reporter.

We next asked whether CCG-1423 binds MICAL-2. To detect CCG-1423 binding to MICAL-2, we used a thermal denaturation assay. In this assay, the melting temperature (T_m) of a protein is measured by increasing the temperature of a sample in the presence of a fluorescent dye, such as 1-anilinonaphthalene-8-sulfonic acid (1,8-ANS) (Pantoliano et al., 2001). As the protein unfolds, 1,8-ANS binds the exposed hydrophobic domains, increasing the dye's fluorescence. Ligand binding is detected by observing an increase or decrease in the T_m. Incubation of MICAL-2 with CCG-1423 decreased the T_m by $-0.3°C$ with an EC_{50} of 3.8 μM. A structurally similar compound with markedly reduced potency at inhibiting SRF/MRTF-A signaling (CCG-100594) (Evelyn et al., 2010) had no significant effect on T_m (Figure 7B, and S7A–S7C), indicating that these effects are specific to CCG-1423. Taken together, these data indicate that CCG-1423 directly binds MICAL-2.

We next asked whether CCG-1423 binding affects MICAL-2 catalytic activity. To test MICAL-2 activity, we used an NADPH depletion assay. Recombinant MICAL-2, comprising the enzymatic domain and the CH domain (MICAL-$2^{redoxCH}$), was incubated with NADPH in the presence of F-actin, and the consumption of NADPH was monitored by UV absorbance. Addition of CCG-1423 (10 μM) markedly reduced NADPH consumption by MICAL-2 compared to CCG-100594 (Figure 7C). CCG-1423 increases the K_m of NADPH and exhibited a K_i of 1.57 μM (Figure 7D). Taken together, these data indicate that CCG-1423 binds MICAL-2 and inhibits its enzymatic activity.

DISCUSSION

Our studies identify redox modification of nuclear actin as a mechanism that mediates the activation of SRF/MRTF-A-dependent gene transcription. We find that MICAL-2 catalyzes the disassembly of nuclear actin polymers, which leads to a reduction in nuclear G-actin levels. This reduction in nuclear G-actin allows MRTF-A to accumulate in the nucleus by impairing its nuclear export, which in turn facilitates SRF/MRTF-A-dependent gene induction. Indeed, expression of MICAL-2 is sufficient to induce SRF/MRTF-A-dependent gene expression. Additionally, knockdown of MICAL-2 markedly reduces NGF-stimulated SRF/MRTF-A-dependent expression and neurite growth. Our findings identify MICAL-2 as a novel regulator of SRF/MRTF-A signaling that acts by regulating nuclear actin.

SRF/MRTF-A-dependent gene transcription can be induced by RhoA-dependent pathways that lead to the sequestration of actin in stress fibers (Miralles et al., 2003; Stern et al., 2009). Our studies identify a mechanism for activation of SRF/MRTF-A-dependent gene transcription which does not involve

(H) *mical2b* knockdown impairs SRF/MRTF-A-dependent, but not SRF/MRTF-A-independent gene transcription. Levels are compared to control wild-type (WT) embryos for the *mical2b* morphants (2B), and in embryos rescued by coinjected RNA encoding the full-length wild-type murine MICAL-2 or the MICAL-2GV mutant protein. Experimental gene levels were normalized by comparison to housekeeping gene EF1α. ANOVA (***$p < 0.0005$) with Dunnett posttest. ***$p < 0.0005$, **$p < 0.005$, **$p < 0.05$, $n \geq 6$. Mean ± SEM.
See also Figure S5 and Table S2.

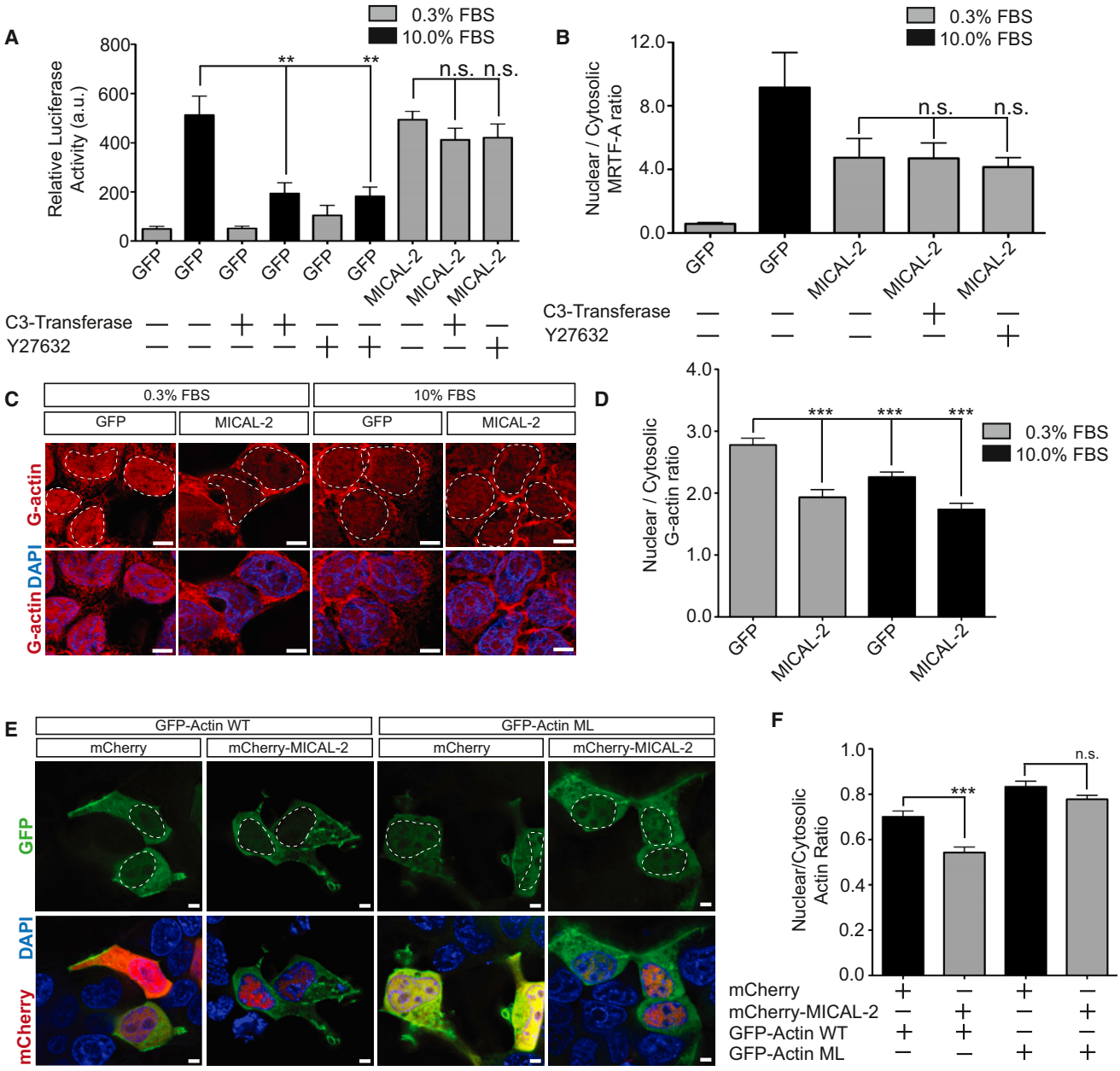

Figure 6. MICAL-2 Regulates Nuclear Actin Independent of RhoA

(A) MICAL-2 induces the SRF/MRTF-A luciferase reporter in a ROCK- and RhoA-independent manner. Treatment with either inhibitor reduced luciferase expression induced by serum-stimulation, but not by MICAL-2 expression. ANOVA (***$p < 0.0001$) with Dunnett posttest. n = 8. All data in this figure are mean ± SEM.

(B) MICAL-2 induces nuclear MRTF-A in a ROCK- and RhoA-independent manner. HEK293T cells were infected with either GFP or GFP-MICAL-2. Nuclear accumulation of MRTF-A was unaffected in MICAL-2 expressing, serum-starved HEK293T cells treated with either 2 μg/ml C3-transferase, a RhoA inhibitor, or 100 μM Y27632, a ROCK inhibitor. ANOVA (***$p < 0.0001$) with Dunnett posttest.

(C) MICAL-2 expression decreases the nuclear to cytosolic ratio of G-actin in HEK293T cells. In starved GFP-expressing cells, G-actin is readily detectable in the nucleus (blue), as measured by DNase I staining (red). Serum stimulation and GFP-MICAL-2 significantly reduced the amount of G-actin in the nucleus. Scale bar, 5 μm.

(D) Quantification of the nuclear:cytosolic DNase I staining seen in C. ANOVA (***$p < 0.0001$) with Dunnett posttest. ***$p < 0.0005$, $n \geq 30$.

(E) MICAL-2 expression reduces nuclear levels of GFP-Actin, but not GFP-actin M44L. When overexpressed, GFP-actin M44L is enriched in the nucleus (blue) when compared to wild-type GFP-Actin. MICAL-2 (red) coexpression further decreases the levels of nuclear wild-type GFP-actin (green) while having no effect on the nuclear levels of GFP-actin M44L. Scale bar, 5 μm.

(F) Quantification of the nuclear:cytosolic GFP-actin staining seen in G. ANOVA (***$p < 0.0001$) with Dunnett posttest. ***$p < 0.0005$, $n \geq 25$.

See also Figure S6.

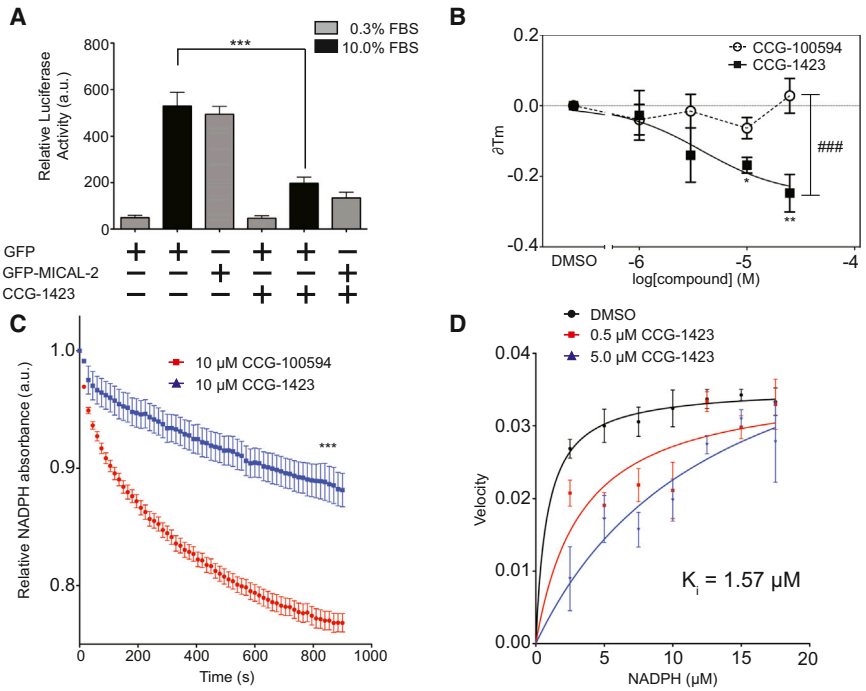

Figure 7. MICAL-2 Is Targeted by CCG-1423

(A) CCG-1423 inhibits MICAL-2-induced activation of the SRF/MRTF-A transcriptional reporter by both serum and MICAL-2 expression. ANOVA (***$p < 0.0001$) with Dunnett posttest. ***$p < 0.0005$, $n = 24$. All data in this figure are mean ± SEM.

(B) CCG-1423 exhibits concentration-dependent thermal destabilization of MICAL2-EN. Recombinant MICAL2-EN, which comprises the enzymatic domain of MICAL-2, was incubated with increasing concentrations of CCG-1423, or the control compound, CCG-100594, and the T_m was calculated in a thermal denaturation assay. Incubation of CCG-1423 exhibited thermal destabilization of MICAL-2 with an IC_{50} of 3.8 μM and Hill coefficient -1.1. ANOVA, Bonferroni's multiple comparisons test *$p < 0.05$ 10 μM 1423 versus DMSO; **$p < 0.01$ 25 μM 1423 versus DMSO; ###, $p < 0.001$ 25 μM 1423 versus 25 μM 100594. 10 μM at $n = 12$ and 25 μM at $n = 7$.

(C) CCG-1423 inhibits MICAL-2 enzymatic activity. We monitored MICAL-2 activity using an NADPH consumption assay. MICAL-2 was incubated with either 5 μM CCG-1423 or the inactive control compound CCG-100594 in the presence of 2 μM F-actin and 10 μM NADPH. ***$p < 0.0005$, Student's t test, $n = 9$.

(D) Enzyme kinetics of MICAL-2. Velocity of recombinant MICAL-2 activity as a function of NADPH and CCG-1423. MICAL-$2^{redoxCH}$ was incubated with DMSO, 0.5 μM or 5 μM CCG-1423. CCG-1423 inhibits MICAL-2 with a K_i of 1.57 μM. See also Figure S7.

regulation of cytosolic actin pathways but which involves regulation of nuclear actin levels. The significance of MICAL-2-dependent activation of SRF/MRTF-A-dependent gene transcription is supported by the impaired nuclear localization of MRTF-A and SRF/MRTF-A-dependent gene transcription in MICAL-2 knockdown PC12 cells, DRG sensory neurons, and HEK293T cells. SRF/MRTF-A-dependent gene transcription in vivo is impaired by knockdown of the zebrafish MICAL-2 ortholog. These studies identify MICAL-2 as a physiologic mediator of SRF/MRTF-A signaling in diverse cell types.

The MICAL-2-mediated increase in nuclear MRTF-A levels appears to be caused by a reduction in nuclear G-actin levels. This is the same mechanism by which stress fiber induction leads to nuclear retention of MRTF-A (Vartiainen et al., 2007). G-actin binds MRTF-A to induce its nuclear export (Miralles et al., 2003; Mouilleron et al., 2011). By reducing nuclear G-actin, MRTF-A loses the cofactor needed for its export, resulting in nuclear accumulation. The ability of MICAL-2 to depolymerize nuclear F-actin originally suggested to us that MICAL-2 would increase nuclear G-actin levels and therefore decrease MRTF-A levels in the nucleus. However, the opposite effect was seen: MICAL-2 expression led to increased nuclear levels of MRTF-A. Furthermore, MICAL-2 expression reduced overall nuclear G-actin levels, to the same degree that is seen following serum and NGF stimulation. Several mechanisms may explain how MICAL-2 activity leads to reduced G-actin in nuclei. Oxidation of actin by MICAL-2 may affect the kinetics of actin import and/or export, as suggested by the different localizations of actin M44L and M44Q. Additionally, MICAL-2-mediated oxidation of actin may alter the binding between MRTF-A and actin. The precise mechanisms by which MICAL-2 activity reduces nuclear actin levels remains to be established.

While MICAL-1 is cytosolic, MICAL-2 and -3 appear to be enriched in the nucleus. MICAL-2 has also been detected in both HeLa cytosol and nucleus by another group; however, this localization was seen using a MICAL-2 overexpression construct (Giridharan et al., 2012). The effects of MICAL-2 that we see in HEK293T cells, PC12 cells, and DRG neurons are unlikely to reflect cytosolic functions of MICAL-2 because MICAL-2 is predominantly nuclear in these cell types and because the effects of MICAL-2 on SRF/MRTF-A-dependent gene transcription are not seen following expression of MICAL-2 constructs that contain mutations in the nuclear-localization sequence. Thus, the effects of MICAL-2 reflect its ability to depolymerize nuclear F-actin.

The proteins that regulate nuclear actin polymerization are poorly understood. In addition to its role in mediating export of MRTF-A from the nucleus, nuclear actin regulates Pol I-mediated transcription of ribosomal RNA genes (rDNA) (Philimonenko et al., 2004), preinitiation complexes necessary for RNA Pol II transcription (Hofmann et al., 2004), and nuclear morphology (Krauss et al., 2003). Therefore, MICAL-2 could influence other actin-mediated pathways as well. MICAL-3, may also have nuclear roles. Although we did not find an effect of MICAL-3 on SRF/MRTF-A-dependent signaling, MICAL-3 may regulate pools of nuclear actin linked to other processes.

The pathways that regulate MICAL-2 activity are not known. MICAL-2 phosphorylation is affected by serum, suggesting that phosphorylation could alter aspects of MICAL-2 function. Additionally, because MICAL-2 uses NADPH to induce F-actin depolymerization, NADPH levels may influence MICAL-2 activity. Indeed, cellular NADPH levels are markedly altered by oncogenic mutations and affect cancer cell growth and metastasis through poorly understood pathways (Dang, 2012). It will be interesting to determine whether these metabolic alterations influence MICAL-2 activity and SRF/MRTF-dependent gene transcription.

Our findings point to MICAL-2 as a target of CCG-1423, an inhibitor of SRF/MRTF-A signaling. CCG-1423 was originally identified in a screen for compounds that inhibit an SRF/MRTF-A transcriptional reporter (Evelyn et al., 2007). However, the molecular target of CCG-1423 has been elusive thus far. We find that CCG-1423 exhibits effects on MRTF-A localization and SRF/MRTF-A reporter expression that resemble the effects seen with MICAL-2 inhibition. Our data suggest that the effects of CCG-1423 are due to inhibition of MICAL-2. Indeed, CCG-1423 binds MICAL-2 at concentrations similar to those that block SRF/MRTF-A signaling in cells (Evelyn et al., 2007; Minami et al., 2012). Importantly, a closely related analog devoid of activity against SRF/MRTF-A signaling shows negligible binding to MICAL-2.

Recent studies have shown that CCG-1423 improves glycemic control in insulin-resistant mice (Jin et al., 2011), prevents fibrosis (Sakai et al., 2013), and reduces metastatic behavior of prostate and melanoma cancer cell lines (Evelyn et al., 2010). Although CCG-1423 has promising effects in preclinical studies, improvements in the potency of CCG-1423 have been challenging (Evelyn et al., 2010), in large part because the specific CCG-1423 target was unknown. Thus, our identification of MICAL-2 as a target of CCG-1423 will facilitate the development of novel inhibitors of SRF/MRTF-A-dependent gene transcription that function by inhibiting MICAL-2 enzymatic activity.

EXPERIMENTAL PROCEDURES

Cell Culture and Reagents

Primers, shRNA, plasmids, cell lines, and antibodies used in this study are listed in Tables S1 and S2 and the Extended Experimental Procedures.

qRT-PCR

Total RNA was prepared using TRIzol (Invitrogen). We synthesized cDNA using Superscript III (Invitrogen) and performed qRT-PCR utilizing iQ SYBR Green Supermix (Bio-rad) and the Realplex Mastercycler ep s (Eppendorf). For a list of primers used see Table S1 and the Extended Experimental Procedures.

Luciferase and MICAL Assays

Activation of SRF/TCF and SRF/MRTF-A-dependent gene transcription was measured using the pGL4.33 and pGL4.34 reporter plasmids, respectively (Promega). Luciferase levels were measured using ONE-glo (Promega) and with a Spectramax L luminometer (Molecular Devices).

Recombinant MICAL-1-, -2- and -3-induced actin depolymerization was measured by monitoring the loss of fluorescence of pyrene-labeled actin (Cytoskeleton) as described previously (Hung et al., 2010). MICAL-1, -2 and -3 activity assays were measured by in an NADPH depletion assay as previously described (Hung et al., 2010). Further details can be found in the Extended Experimental Procedures.

Zebrafish

Wild-type zebrafish (AB/Tu hybrid strain) were maintained as described (Westerfield, 1993). Transgenic reporter strain tg(*myl7:egfp*) was obtained from ZIRC, and tg(*myl7:actn3b-egfp*) was kindly provided by D. Yelon (UCSD). Morpholinos were purchased from Genetools. Sequences and experimental details can be found in the Extended Experimental Procedures and Table S2.

SUPPLEMENTAL INFORMATION

Supplemental Information includes Extended Experimental Procedures, seven figures, and two tables and can be found with this article online at http://dx.doi.org/10.1016/j.cell.2013.12.035.

ACKNOWLEDGMENTS

We thank A. Deglincerti and members of the Jaffrey lab for helpful comments and suggestions. This work was supported by NIH grants F32AT4340 (M.R.L.), HL111400 (T.E.), and NS56306 (S.R.J.).

Received: December 31, 2012
Revised: September 23, 2013
Accepted: November 12, 2013
Published: January 16, 2014

REFERENCES

Baarlink, C., Wang, H., and Grosse, R. (2013). Nuclear actin network assembly by formins regulates the SRF coactivator MAL. Science *340*, 864–867.

Brandt, D.T., Baarlink, C., Kitzing, T.M., Kremmer, E., Ivaska, J., Nollau, P., and Grosse, R. (2009). SCAI acts as a suppressor of cancer cell invasion through the transcriptional control of beta1-integrin. Nat. Cell Biol. *11*, 557–568.

Buchwalter, G., Gross, C., and Wasylyk, B. (2004). Ets ternary complex transcription factors. Gene *324*, 1–14.

Chong, N.W., Koekemoer, A.L., Ounzain, S., Samani, N.J., Shin, J.T., and Shaw, S.Y. (2012). STARS is essential to maintain cardiac development and function in vivo via a SRF pathway. PLoS ONE *7*, e40966.

Chun, L.L., and Patterson, P.H. (1977). Role of nerve growth factor in the development of rat sympathetic neurons in vitro. I. Survival, growth, and differentiation of catecholamine production. J. Cell Biol. *75*, 694–704.

Dang, C.V. (2012). Links between metabolism and cancer. Genes Dev. *26*, 877–890.

Davis, J.L., Long, X., Georger, M.A., Scott, I.C., Rich, A., and Miano, J.M. (2008). Expression and comparative genomics of two serum response factor genes in zebrafish. Int. J. Dev. Biol. *52*, 389–396.

Descot, A., Hoffmann, R., Shaposhnikov, D., Reschke, M., Ullrich, A., and Posern, G. (2009). Negative regulation of the EGFR-MAPK cascade by actin-MAL-mediated Mig6/Errfi-1 induction. Mol. Cell *35*, 291–304.

Eppink, M.H.M., Schreuder, H.A., and Van Berkel, W.J. (1997). Identification of a novel conserved sequence motif in flavoprotein hydroxylases with a putative dual function in FAD/NAD(P)H binding. Protein Sci. *6*, 2454–2458.

Evelyn, C.R., Wade, S.M., Wang, Q., Wu, M., Iñiguez-Lluhí, J.A., Merajver, S.D., and Neubig, R.R. (2007). CCG-1423: a small-molecule inhibitor of RhoA transcriptional signaling. Mol. Cancer Ther. *6*, 2249–2260.

Evelyn, C.R., Bell, J.L., Ryu, J.G., Wade, S.M., Kocab, A., Harzdorf, N.L., Hollis Showalter, H.D., Neubig, R.R., and Larsen, S.D. (2010). Design, synthesis and prostate cancer cell-based studies of analogs of the Rho/MKL1 transcriptional pathway inhibitor, CCG-1423. Bioorg. Med. Chem. Lett. *20*, 665–672.

Giridharan, S.S.P., Rohn, J.L., Naslavsky, N., and Caplan, S. (2012). Differential regulation of actin microfilaments by human MICAL proteins. J. Cell Sci. *125*, 614–624.

Hofmann, W.A., Stojiljkovic, L., Fuchsova, B., Vargas, G.M., Mavrommatis, E., Philimonenko, V., Kysela, K., Goodrich, J.A., Lessard, J.L., Hope, T.J., et al. (2004). Actin is part of pre-initiation complexes and is necessary for transcription by RNA polymerase II. Nat. Cell Biol. *6*, 1094–1101.

Hung, R.-J., Yazdani, U., Yoon, J., Wu, H., Yang, T., Gupta, N., Huang, Z., van Berkel, W.J.H., and Terman, J.R. (2010). Mical links semaphorins to F-actin disassembly. Nature *463*, 823–827.

Hung, R.-J., Pak, C.W., and Terman, J.R. (2011). Direct redox regulation of F-actin assembly and disassembly by Mical. Science *334*, 1710–1713.

Jin, W., Goldfine, A.B., Boes, T., Henry, R.R., Ciaraldi, T.P., Kim, E.-Y., Emecan, M., Fitzpatrick, C., Sen, A., Shah, A., et al. (2011). Increased SRF transcriptional activity in human and mouse skeletal muscle is a signature of insulin resistance. J. Clin. Invest. *121*, 918–929.

Knöll, B., and Nordheim, A. (2009). Functional versatility of transcription factors in the nervous system: the SRF paradigm. Trends Neurosci. *32*, 432–442.

Krauss, S.W., Chen, C., Penman, S., and Heald, R. (2003). Nuclear actin and protein 4.1: essential interactions during nuclear assembly in vitro. Proc. Natl. Acad. Sci. USA *100*, 10752–10757.

Lee, S.-M., Vasishtha, M., and Prywes, R. (2010). Activation and repression of cellular immediate early genes by serum response factor cofactors. J. Biol. Chem. *285*, 22036–22049.

Leitner, L., Shaposhnikov, D., Mengel, A., Descot, A., Julien, S., Hoffmann, R., and Posern, G. (2011). MAL/MRTF-A controls migration of non-invasive cells by upregulation of cytoskeleton-associated proteins. J. Cell Sci. *124*, 4318–4331.

Li, S., Chang, S., Qi, X., Richardson, J.A., and Olson, E.N. (2006). Requirement of a myocardin-related transcription factor for development of mammary myoepithelial cells. Mol. Cell. Biol. *26*, 5797–5808.

Liang, D., Chang, J.R., Chin, A.J., Smith, A., Kelly, C., Weinberg, E.S., and Ge, R. (2001). The role of vascular endothelial growth factor (VEGF) in vasculogenesis, angiogenesis, and hematopoiesis in zebrafish development. Mech. Dev. *108*, 29–43.

Lu, P.P.Y., and Ramanan, N. (2011). Serum response factor is required for cortical axon growth but is dispensable for neurogenesis and neocortical lamination. J. Neurosci. *31*, 16651–16664.

Medjkane, S., Perez-Sanchez, C., Gaggioli, C., Sahai, E., and Treisman, R. (2009). Myocardin-related transcription factors and SRF are required for cytoskeletal dynamics and experimental metastasis. Nat. Cell Biol. *11*, 257–268.

Minami, T., Kuwahara, K., Nakagawa, Y., Takaoka, M., Kinoshita, H., Nakao, K., Kuwabara, Y., Yamada, Y., Yamada, C., Shibata, J., et al. (2012). Reciprocal expression of MRTF-A and myocardin is crucial for pathological vascular remodelling in mice. EMBO J. *31*, 4428–4440.

Miralles, F., Posern, G., Zaromytidou, A.-I., and Treisman, R. (2003). Actin dynamics control SRF activity by regulation of its coactivator MAL. Cell *113*, 329–342.

Mouilleron, S., Langer, C.A., Guettler, S., McDonald, N.Q., and Treisman, R. (2011). Structure of a pentavalent G-actin*MRTF-A complex reveals how G-actin controls nucleocytoplasmic shuttling of a transcriptional coactivator. Sci. Signal. *4*, ra40.

Pantoliano, M.W., Petrella, E.C., Kwasnoski, J.D., Lobanov, V.S., Myslik, J., Graf, E., Carver, T., Asel, E., Springer, B.A., Lane, P., and Salemme, F.R. (2001). High-density miniaturized thermal shift assays as a general strategy for drug discovery. J. Biomol. Screen. *6*, 429–440.

Philimonenko, V.V., Zhao, J., Iben, S., Dingová, H., Kyselá, K., Kahle, M., Zentgraf, H., Hofmann, W.A., de Lanerolle, P., Hozák, P., and Grummt, I. (2004). Nuclear actin and myosin I are required for RNA polymerase I transcription. Nat. Cell Biol. *6*, 1165–1172.

Posern, G., and Treisman, R. (2006). Actin' together: serum response factor, its cofactors and the link to signal transduction. Trends Cell Biol. *16*, 588–596.

Riedl, J., Crevenna, A.H., Kessenbrock, K., Yu, J.H., Neukirchen, D., Bista, M., Bradke, F., Jenne, D., Holak, T.A., Werb, Z., et al. (2008). Lifeact: a versatile marker to visualize F-actin. Nat. Methods *5*, 605–607.

Rost, B., Yachdav, G., and Liu, J. (2004). The PredictProtein server. Nucleic Acids Res. *32* (Web Server issue), W321–W326.

Sakai, N., Chun, J., Duffield, J.S., Wada, T., Luster, A.D., and Tager, A.M. (2013). LPA1-induced cytoskeleton reorganization drives fibrosis through CTGF-dependent fibroblast proliferation. FASEB J. *27*, 1830–1846.

Selvaraj, A., and Prywes, R. (2004). Expression profiling of serum inducible genes identifies a subset of SRF target genes that are MKL dependent. BMC Mol. Biol. *5*, 13.

Shaw, P.E., Schröter, H., and Nordheim, A. (1989). The ability of a ternary complex to form over the serum response element correlates with serum inducibility of the human c-fos promoter. Cell *56*, 563–572.

Stern, S., Debre, E., Stritt, C., Berger, J., Posern, G., and Knöll, B. (2009). A nuclear actin function regulates neuronal motility by serum response factor-dependent gene transcription. J. Neurosci. *29*, 4512–4518.

Suck, D., Kabsch, W., and Mannherz, H.G. (1981). Three-dimensional structure of the complex of skeletal muscle actin and bovine pancreatic DNAse I at 6-A resolution. Proc. Natl. Acad. Sci. USA *78*, 4319–4323.

Terman, J.R., Mao, T., Pasterkamp, R.J., Yu, H.-H., and Kolodkin, A.L. (2002). MICALs, a family of conserved flavoprotein oxidoreductases, function in plexin-mediated axonal repulsion. Cell *109*, 887–900.

Treisman, R. (1986). Identification of a protein-binding site that mediates transcriptional response of the c-fos gene to serum factors. Cell *46*, 567–574.

Vartiainen, M.K., Guettler, S., Larijani, B., and Treisman, R. (2007). Nuclear actin regulates dynamic subcellular localization and activity of the SRF cofactor MAL. Science *316*, 1749–1752.

Wang, D.-Z., Li, S., Hockemeyer, D., Sutherland, L., Wang, Z., Schratt, G., Richardson, J.A., Nordheim, A., and Olson, E.N. (2002). Potentiation of serum response factor activity by a family of myocardin-related transcription factors. Proc. Natl. Acad. Sci. USA *99*, 14855–14860.

Wang, Z., Wang, D.-Z., Pipes, G.C.T., and Olson, E.N. (2003). Myocardin is a master regulator of smooth muscle gene expression. Proc. Natl. Acad. Sci. USA *100*, 7129–7134.

Westerfield, M. (1993). The zebrafish book: A guide for the laboratory use of zebrafish (Brachydanio rerio) (Eugene: Inst of Neuro Science).

Wickramasinghe, S.R., Alvania, R.S., Ramanan, N., Wood, J.N., Mandai, K., and Ginty, D.D. (2008). Serum response factor mediates NGF-dependent target innervation by embryonic DRG sensory neurons. Neuron *58*, 532–545.

Xue, Y., Kuok, C., Xiao, A., Zhu, Z., Lin, S., and Zhang, B. (2010). Identification and expression analysis of mical family genes in zebrafish. J. Genet. Genomics *37*, 685–693.

Znosko, W.A., Yu, S., Thomas, K., Molina, G.A., Li, C., Tsang, W., Dawid, I.B., Moon, A.M., and Tsang, M. (2010). Overlapping functions of Pea3 ETS transcription factors in FGF signaling during zebrafish development. Dev. Biol. *342*, 11–25.